文章编号:1006-9941(2020)04-0317-13

Crystal Morphology of β-HMX Under Eight Solvents System Using Molecular Dynamics Simulation and Experiment

WANG Lei[1,2], **CHEN Dong**[2], **LI Hong-zhen**[2], **DUAN Xiao-hui**[3], **YU Yan-wu**[1]

(1. *School of Environmental and Safety Engineering, North University of China, Taiyuan* 030051, *China*; 2. *Institute of Chemical Materials, China Academy of Engineering Physics, Mianyang*621999, *China*; 3. *Southwest University of Science and Technology, Mianyang* 621900, *China*)

Abstract: The crystal morphologies of β-HMX (octahydro-1,3,5,7-tetranitro-1, 3, 5, 7-tetrazocine) in eight pure organic solvents were predicted based on the modified attachment energy (AE) model by using molecular dynamics (MD) method. Results demonstrate that the morphological dominant crystal faces of β-HMX in vacuum are: (0 1 1), (1 1 −1), (0 2 0), (1 0 0) and (1 0 −2), respectively. The (1 0 0) face is the most polar crystal face and has the largest interaction energy with the solvent molecules, which results in a slow growth rate and appears as dominant face in the final crystal morphology. The (1 0 −2) and (0 2 0) faces have the small interaction energies with the solvent molecules, which appear as small areas or even disappear in the final crystal morphology. The order of the aspect ratio of the crystal morphology is: cyclopentanone>cyclohexanone>*N*, *N*-dimethylacetamide (DMAC) >pyridine>acetone>triethyl phosphate>propylene carbonate>Dimethyl sulfoxide (DMSO), which indicates that DMSO and propylene carbonate are more favorable for the spheroidization of β-HMX in crystallization experiments. The experimental crystal morphologies of β-HMX in eight pure organic solvents were investigated using a natural cooling recrystallization method. Results show that the predicted morphologies are in good agreement with the experimental results. The attached energy (AE) model is suitable for predicting the crystal morphology of β-HMX, which may serve as a guide in β-HMX recrystallization experiments.

Key words: attached energy(AE)model;β-HMX;crystal morphology;molecular dynamics;simulation

CLC number: TJ55; O64 **Document code**: A **DOI**: 10.11943/CJEM2020019

1 Introduction

Crystal morphology is very important in many fields because the different crystal morphologies will determine filterability, drying and flowability, scalability and storability of a material, and can indirectly affect the end-use properties of the material[1], such as formulation. For explosives, additional demands are placed on their hazardous properties, such as impact and friction sensitivity, thermal stability, and charge processing methods. Besides, the crystal morphology also influences the solid content of the charging process[2-5]. And these significantly affect the weapon's final application system performance include functional force, detonation performances, safety, mechanical properties, ballistic performance and etc[6]. In general, explosive crystals with a smaller aspect ratio (such as bulk, columnar, and spheroidal crystals) have better diffusivity and low sensitivity, which can significantly improve the safety performance and solid-phase content[6-8]. Therefore, the investigation on crystal morphology control of explosives has great value for its further applications.

The crystal morphology of explosives is greatly affected by the crystallization conditions, such as

Received Date: 2020-01-20; **Revised Date**: 2020-02-19

Published Online: 2020-03-09

Project Supported: National Natural Science Foundation of China (21875231)

Biography: WANG Lei (1993-), female, master, research field: crystallization of energetic material. e-mail: 1065003120@qq.com

Corresponding author: YU Yan-wu (1977-), male, associate Professor, research field: application technology and methods of energetic materials. e-mail: yuyanwu11@sina.com

引用本文:王蕾,陈东,李洪珍,等. 八种溶剂体系中HMX晶体形貌的分子动力学模拟和实验研究[J]. 含能材料,2020,28(4):317-329.

WANG Lei, CHEN Dong, LI Hong-zhen, et al. Crystal Morphology of β-HMX Under Eight Solvents System Using Molecular Dynamics Simulation and Experiment [J]. *Chinese Journal of Energetic Materials (Hanneng Cailiao)*, 2020, 28(4):317-329.

solvents, additives, super-saturation and the growth kinetics during crystallization[9]. Among them, the influence of solvent molecules on the crystal morphology is enormous[10], which can be accomplished by experiments and molecular dynamics simulation. Up to now, there are many calculation methods of crystal morphology reported in literatures, such as Bravais-Friedel Donnay-Harker (BFDH) rule[11-13], the periodic bonded chain (PBC) theory[14], Occupancy Model[1] and the modified attachment energy (AE) model[15-20]. In calculating the crystal habit of explosive compounds, the modified AE model is the most commonly used and guaranteed prediction method. For example, Han et al[21].. studied the effects of four solvents such as methanol, ethanol, ethyl acetate and acetone on the morphology of CL-20 crystals Song et al[22].. used the attached energy (AE) model to calculate the crystal morphology of 3, 4-Dinitro-1H-pyrazole (DNP) in different solvents (ethyl acetate, water, water/EtOH and water/AcOH) All these examples mentioned above illustrated that the AE model is effective in predicting the crystal morphology of explosives[23-24].

HMX is high energy explosive with excellent detonation performance and thermal stability[25], and extensively used as energy ingredient in polymer-bonded explosives (PBXs), solid propellants, and so on. HMX has four solid-phase polymorphs, labeled as α, β, γ, δ-HMX[26]. The β-HMX is the stable form and most commonly used in industry due to its highest crystal density, lowest mechanical sensitivity. The crystal morphology of β-HMX has a great influence on its application and performance. Ilana G et al.[27] obtained prismatic, flake-like and needle-like HMX by slow evaporation in a single or binary solvent. Leif S[28], van der Heijden[29] and Kriber H[3] obtained prismatic HMX in γ-butyrolactone and propylene carbonate by cooling method. In the reported literature on theoretical calculations, Duan et al[30-31]. and Yan et al.[32] studied the effect of solvents on the morphology of HMX crystals and successfully predicted the crystal morphology of HMX in acetone and acetonitrile, respectively. Chen et al.[33] also predicted the crystal morphology of HMX in a mixed solvent such as acetone/γ-butyrolactone, DMF/H_2O and acetone-ethyl acetate-water ternary system. There are limited several solvents used for crystallization and lack of the influence relationship of solvents on HMX crystal morphology. However, HMX can be dissolved in many solvents and different solvents have a great influence on the crystals morphology. Therefore, it is very important and necessary to systematically investigate the effects of different solvents on the morphology of HMX, which may guide the modification of HMX crystal morphology and greatly improve efficiency.

In this study, the crystal morphology of HMX in vacuum and eight commonly pure organic solvents with certain solubility, including dimethyl dulfoxide (DMSO), acetone, triethyl phosphate, propylene carbonate, *N*, *N*-dimethylacetamide (DMAC), cyclopentanone, cyclohexanone and pyridine, were predicted by the modified attachment energy (AE) model and molecular dynamics (MD) method. The important factors affecting the morphology of HMX crystals are analyzed at the molecular level. Furthermore, the aspect ratios of different crystal morphologies obtained from the simulation results were calculated and compared, and the spheroidization degree of HMX was quantitatively characterized. Finally, the recrystallization experiment of HMX in the above pure organic solvents have conducted.

2 Predicted model and simulation details

2.1 Attachment energy model

The attached energy (AE) model has been widely used to predict the crystal morphology of explosives and medicine[34]; it was put forward by Hartman based on the periodic bond chain (PBC) theory[15]. The AE model fully considers the crystal unit in the prediction process, and the system energy is more stable. Therefore, the AE model is more accurate than the BFDH method. The attachment energy can be defined as the energy released when the crys-

tal flakes is attached to the surface of a growing crystal face, expressed as E_{att}[19], which can be calculated as Eq (1). The AE model predicts crystal morphology by analyzing the 1/2 symmetry plane distance of the crystal and the distance is related to the linear growth rate of the crystal face, as shown in Eq(2).

$$E_{att} = E_{latt} - E_{slice} \quad (1)$$

$$R_{hkl} \propto E_{att} \quad (2)$$

Where E_{latt} is the crystal lattice energy (kJ·mol^{-1}), and E_{slice} is the energy (kJ·mol^{-1}) released by a wafer growth with a thickness of d_{hkl}. R_{hkl} is the relative linear growth rate of crystal faces (h k l) in a vacuum, which is proportional to its attachment energy.

When the crystal grows in solution, the crystal morphology is affected by the different adsorption interactions between solvent molecules and different faces of the crystal. Therefore, the solvents play an important role in the process of crystal growth and the final crystal morphology. If the stronger the adsorption interaction between the solvent molecule and a certain face of the crystal, the easier the formation of the solvation layer by the solvent molecules adsorbed at the crystal face, therefore, the growth of the corresponding crystal face is suppressed[35]. The growth of the crystal faces has to remove solvent molecules adsorbed on the crystal face, and the energy will be lost during the de-solvation process. The attachment energy decreases on the different crystal faces of the crystal, thus, the crystal morphology cultured in the solution is changed compared with that in the vacuum. The interaction energy between the solvent layer and the crystal face E_{int} can be calculated by Eq.(3):

$$E_{int} = E_{tot} - E_{surf} - E_{solv} \quad (3)$$

Where E_{tot} is the total energy of the solvent and the crystal face, E_{surf} is the energy of crystal face without solvent layer, and E_{solv} is the energy of the solvent layer without the crystal face.

The binding energy of the crystal face in the unit cell with solvent layer expressed as E_s. E_s can be introduced as an energy correction term to correct the attachment energy on the vacuum model, which can be calculated by Eq.(4):

$$E_s = E_{int} \times \frac{A_{acc}}{A_{box}} \quad (4)$$

Where A_{acc} is the area of the crystal face (h k l) in the unit cell, and A_{box} is the total crystal face area of the simulated model along the crystal face (h k l).

We defined the solvent-effected attachment energy as E_{att}', which can be calculated according to the following Eq.(5).

$$E_{att}' = E_{att} - E_s \quad (5)$$

The modified morphological theory proposed by Hartman is based on the relative growth rate of each surface (R_{hkl}') proportional to the absolute value of E_{att}', as shown in Eq.(6).

$$R_{hkl}' \propto E_{att}' \quad (6)$$

The crystal face with the lowest attachment energy has the greatest influence on the overall morphology of the crystal, because it has the slowest growth rate and becomes the dominant crystal face of the crystal.

2.2 Computational details

All simulations in this work were performed using Materials Studio (version 8, Accelrys Inc., USA). The COMPASS force field in the simulation was selected to predict the structure of HMX crystal. The COMPASS force field has proven to be a powerful *ab* initio force field that can be parameterized based on extensive experimental data[36]. The parameterized COMPASS force field can accurately simulate thermo-physical properties and structure of various condensed-phase materials, especially for energetic materials.

The initial structural file of HMX, used in the calculation of this work, is from the reported literature[37] including the lattice parameters a = 6.540 Å, b = 11.050 Å, c=8.700 Å and the space group $P2_1/c$. A simple schematic diagram of the entire simulation process taking DMAC and HMX as an example is shown in Fig. 1. The molecular and unit cell structures of HMX are displayed in Fig. 2a and Fig. 2b. Firstly, the initial crystal structure of the HMX was optimized using the *Forcite* module in MS. The morphology of the HMX crystal under vacuum condi-

tions was simulated by the AE model, and the morphologically important surface (h k l) was obtained. The results show that the crystal of HMX in vacuum has five important faces, which is (0 1 1), (0 2 0), (1 1 −1), (1 0 0) and (1 0 −2), respectively. The above five important crystal faces were cut out by "cleave" and "super-cell", and the periodic superstructure of each important crystal face of length and width approximately 30 Å was constructed. The operations on the above five important crystal faces are consistent. Secondly, the solvent layers were constructed by the Amorphous Cell module, which had 300 randomly distributed solvent molecules at the target density of each solvent. The size of the solvent box is determined by the size of each periodic superstructure. Third, the HMX crystal face-solvent molecule adsorption model of important face (h k *l*) was constituted by each important face and the corresponding different solvent boxes. In the established adsorption model, a vacuum layer with thickness 40 Å was created above the solvent layer in order to eliminate the effects of additional free boundaries. The HMX crystal face-solvent molecule adsorption model of each important face (h k *l*) was optimized using the *Forcite* module. Finally, the MD simulations were performed in an NVT ensemble with a temperature of 298 ℃ under the Anderson thermostat for the uniform distribution of solvent molecules.

The calculations for electrostatic non-bond interactions were performed by using the standard E_{wald} method with a calculation accuracy of 0.418 J·mol^{-1}, and the calculation of Van der Waals forces (VdW) is based on *atom-based* summation. The molecular dynamics calculation was carried out on the geometrically optimized HMX crystal face-solvent molecular adsorption model, using an NVT ensemble with a temperature of 298 ℃. The balanced run was performed with a total simulation time of 200 ps and a time step of 1 fs, during which data was collected every 20,000 steps for subsequent analysis.

3 Experimental section

3.1 Materials and characterization

HMX is a compound with molecular mass of 296.16 and the CAS registry NO.2691-41-0, and its purity is 99.5%, determined by high performance liquid chromatography (HPLC, UltiMate3000DGLC). In this work, The HMX used comes from Institute of Chemical Materials, CAEP. DMSO, acetone

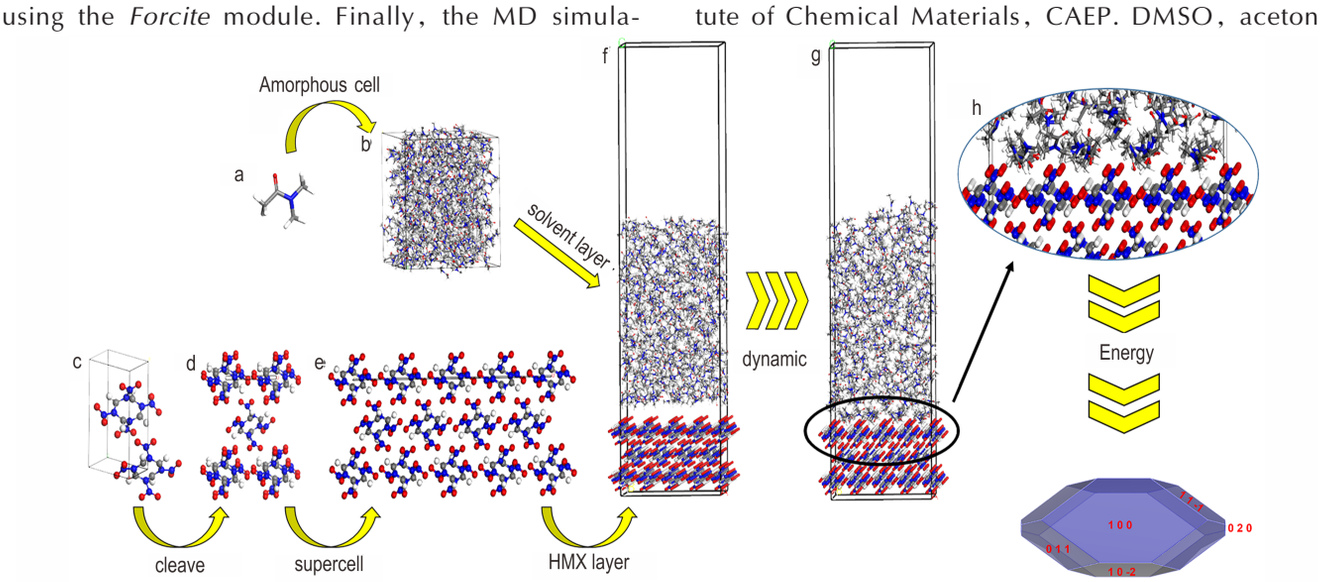

Fig.1 A simple schematic diagram of the entire simulation process taking DMAC and HMX (0 2 0) as an example
a—DMAC molecule, b—Amorphous solvent box, c—HMX unit cell, d—One of the important surfaces of HMX (0 2 0), e—The super cell of (0 2 0), f—The two-layer structure model of (0 2 0) and the amorphous solvent box of DMAC, g—The balanced state after dynamic of the two-layer structure model, h—Solvent molecules adsorbed on the crystal face, i—the crystal morphology of HMX affect by DMAC molecules

and triethyl phosphate used are from Tianjin Chemical Industry Co., Ltd. Propylene Carbonate, cyclopentanone and cyclohexanone were produced in Chengdu United Institute of Chemical & Reagent. DMAC and pyridine are from Sinopharm Chemical Reagent Co., Ltd. The purity of all solvents used was greater than 99.0%. The scanning electron microscopy (SEM) images of HMX crystals were obtained using a ZEISS sigma-HD-0129 operated at an acceleration voltage of 3 kV. The power X-ray diffraction (PXRD) patterns were determined by Bruker D8 ADVANCE X-ray powder diffractometer.

3.2 Recrystallization

All of the recrystallized samples of HMX in solvents were obtained by the natural cooling method. Firstly, 20 mL of solvent and excess HMX were added to a 50 mL round bottom flask, and the solution was heated from room temperature to 85 ℃ (acetone at 50 ℃) in an oil bath and stirred at 300 r·min^{-1} for 2 h to ensure the formation of a solution mixture containing excess HMX solids. After that, the saturated supernatant was taken out and placed in a 50 mL vial, cooled down to room temperature at a certain rate, subjected to suction filtration and dried at 60 ℃ to obtain the recrystallized samples of HMX. The heated magnetic stirrer (1KIA, RET control-visc) was used to control the temperature and agitation speed of the entire experimental system.

4 Results and discussion

4.1 HMX crystal morphology in vacuum

The crystal morphology of HMX in vacuum was simulated by the AE model, and the parameter information of five important crystal faces (h k *l*) of HMX ideal crystal was calculated and shown in Table 1. Especially, the area of each important crystal face and the proportion in the crystal are more intuitive as shown in Fig.2. The aspect ratio of HMX simulated by the AE model in vacuum is 1.934, and the aspect ratio reported in the literature is 2.06[30]. The difference may be caused by different simulation conditions. In the reported literature, simulations were

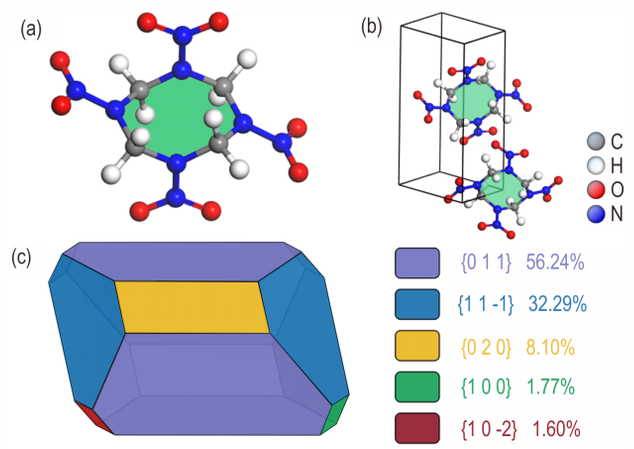

Fig.2 The crystal morphology of HMX in vacuum simulated by the AE model

a—The molecular structure of HMX, b—The cell structure of HMX, c—The crystal morphology of HMX in vacuum simulated by the AE model

performed using 200 solvent molecules at a simulation temperature of 276.85 ℃ (550 K) and a total simulation time of 140 ps. In this work, 300 solvent molecules were used to simulate at a simulation temperature of 298 ℃ and a total simulation time of 200 ps. The results show that there are five important surfaces (h k *l*) in the ideal crystal of HMX, which are (0 1 1), (1 1 −1), (0 2 0), (1 0 0) and (1 0 −2). Among them, the morphological importance of the (0 1 1) is the strongest, which has the largest inter-planar distance ($d_{(0\,1\,1)}$=6.025 Å) and the biggest proportion area in the crystal (Total facet area$_{(0\,1\,1)}$= 56.237%). The absolute value of attachment energy of (0 1 1) is minimum with 110.083 kJ·mol^{-1}, including Van der Waals force (VdW) −83.627 kJ·mol^{-1} and electrostatic potential energy −26.456 kJ·mol^{-1}. And, the (1 0 −2) plane is the lowest important crystal face in the crystal, the total facet area is only 1.605% and the minimum growth distance is 4.317 Å. The information of other important crystal faces was listed in Table 1.

Futherly, the surface chemistry of the important crystal faces was analyzed to study the adsorption of solvent molecules on various important crystal faces. And the molecular arrangement and the Connolly surface of the HMX ideal morphology in vacuum was obtained as shown in Fig.3. In Fig.3, the purple

Table 1 Calculate attachment energies for dominant crystal habit faces and other information simulated by AE model in vacuum

h k l[1)]	multiplicity	d_{hkl}[2)]	R[3)]	E_{att}(total)	E_{att}(VdW)	E_{att}(electrostatic)	distance	total facet area	total facet area/%
(0 1 1)	4	6.025	1	−110.083	−83.627	−26.456	26.293	10595.28	56.237
(0 2 0)	2	5.525	1.340	−147.546	−89.316	−58.229	35.241	1526.990	8.105
(1 1 −1)	4	5.523	1.396	−153.676	−96.543	−57.137	36.705	6082.869	32.286
(1 0 0)	2	5.403	1.880	−206.953	−125.909	−81.043	49.430	332.894	1.767
(1 0 −2)	2	4.317	1.548	−170.360	−107.969	−62.391	40.690	302.373	1.605

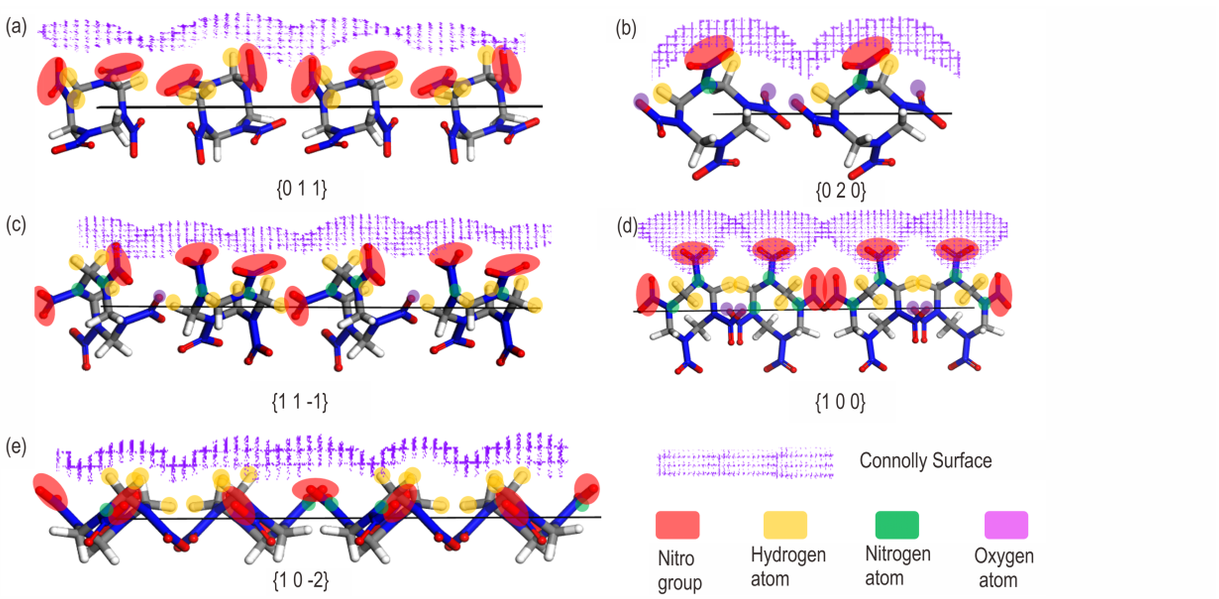

Fig.3 Molecular arrangement and Connolly surface of the crystal face of HMX

grid on the surfaces indicates the Connolly surface. Obviously, (1 0 0) is the roughest surface because the nitro group are directly exposed and perpendicular to the surface. Secondly, the relatively smooth surfaces are (1 1 −1), (0 2 0) and (0 1 1), and their nitro, hydrogen, oxygen and nitrogen atoms are exposed at different positions and angles on the surface. (1 0 −2) is the smoothest surface and only the hydrogen atoms are exposed on the surface and the nitro groups are paralleled to the surface. The value of S is the ratio of the solvent accessible area (A_{acc}) on the unit crystal face to the corresponding unit crystal face area (A_{hkl})[21], which defined as Eq (7).

$$S = \frac{A_{acc}}{A_{hkl}} \tag{7}$$

The parameters S listed in Table 2 can quantitatively indicate the difference in the step structures and surface chemistry of the important crystal surfaces. It can be seen from Table 2, the S value of (1 0 0) is 1.907, which is the largest among the five important crystal surfaces. This means that the (1 0 0) surface is most exposed to the solvent, and the roughest, which is favorable for the adsorption of solvent molecules. For (1 1 −1), (0 2 0), and (0 1 1), the S values are not much different. The S value of (1 0 −2) is the smallest, which indicates that the surface is the flattest and the proportion of solvent molecules contacted on the surface is the smallest. Based on the above analysis, the relative polarity order of the five important crystal surfaces is: (1 0 0)>(1 1 −1)>(0 2 0)>(0 1 1)>(1 0 −2).

Table 2 Surface areas for the important crystal surfaces and the value of parameter S[1)]

surface	(0 1 1)	(0 2 0)	(1 1 −1)	(1 0 0)	(1 0 −2)
A_{acc}[2)]/Å^2	109.933	62.213	126.021	183.316	132.737
A_{hkl}[3)]/Å^2	96.208	47.003	94.041	96.135	120.299
S	1.276	1.324	1.340	1.907	1.103

Note: 1) The value of S quantitatively indicate the difference in the step structures of the important crystal surfaces. 2) Connolly surface area exposed to solvent in unit cell. 3) The surface area of the important crystal face (h k l) in unit cell.

4.2 HMX crystal morphology in solvents

The adsorption characteristics of solvent molecules on the important crystal surfaces of HMX can be analyzed from the adsorption behavior of different solvent molecules on a same important crystal surface. Taking (0 1 1) crystal surface as an example, a series of (0 1 1)-solvent molecule adsorption models were constructed with DMSO, acetone, triethyl phosphate, propylene carbonate, DMAC, cyclopentanone, cyclohexanone and pyridine. The equilibrium configurations of the (0 1 1)-solvent molecule adsorption model structures are simulated as shown in Fig.4. It can be seen from Fig.5, that the solvent molecules are constantly approaching the (0 1 1) surface of the HMX crystal with different distances. This phenomenon is caused by the mutual attraction between the solvent molecules and the polar groups exposed on the (0 1 1) surfacedue to the nitro groups. It can be seen that the binding degree of DMSO molecule to (0 1 1) is the closest, which has the largest interaction energy (E_{int}=−557.346 kJ·mol^{-1}) and solvent binding energy (E_s=−88.889 kJ·mol^{-1}). The negative sign of all mentioned energy indicates the interaction between the solvent and the crystal surface is absorption. The interaction energy (E_{int}) and the solvent binding energy (E_s) of pyridine to the (0 1 1) crystal surface is the smallest, which is 1.297 kJ·mol^{-1} and 0.205 kJ·mol^{-1}, respectively. Table 3 shows that the order of the interaction energy (E_{int}) and the solvent binding energy (E_s) of the (0 1 1) crystal surface with different solvent molecules is: DMSO>DMAC>triethyl phosphate>propylene carbonate>cyclohexanone>cyclopentanone>acetone>pyridine. For the (0 1 1) crystal surface, the solvent binding energy increases with the increase of the polarity of the solvents, and adsorption behavior of the other four surface-solvent molecule adsorption models is basically the same as that of (0 1 1).

The adsorption characteristics of solvent molecules on the important crystal surfaces of HMX can be analyzed from the adsorption behavior of the same solvent molecule on five important crystal surfaces. Taking DMSO as an example, the different adsorption effects of solvents on the five important crystal surfaces of HMX were analyzed. Under the influence of DMSO, the morphology of HMX and the attachment energy of the five important crystal surfaces have changed. The interaction energy (E_{int}) and

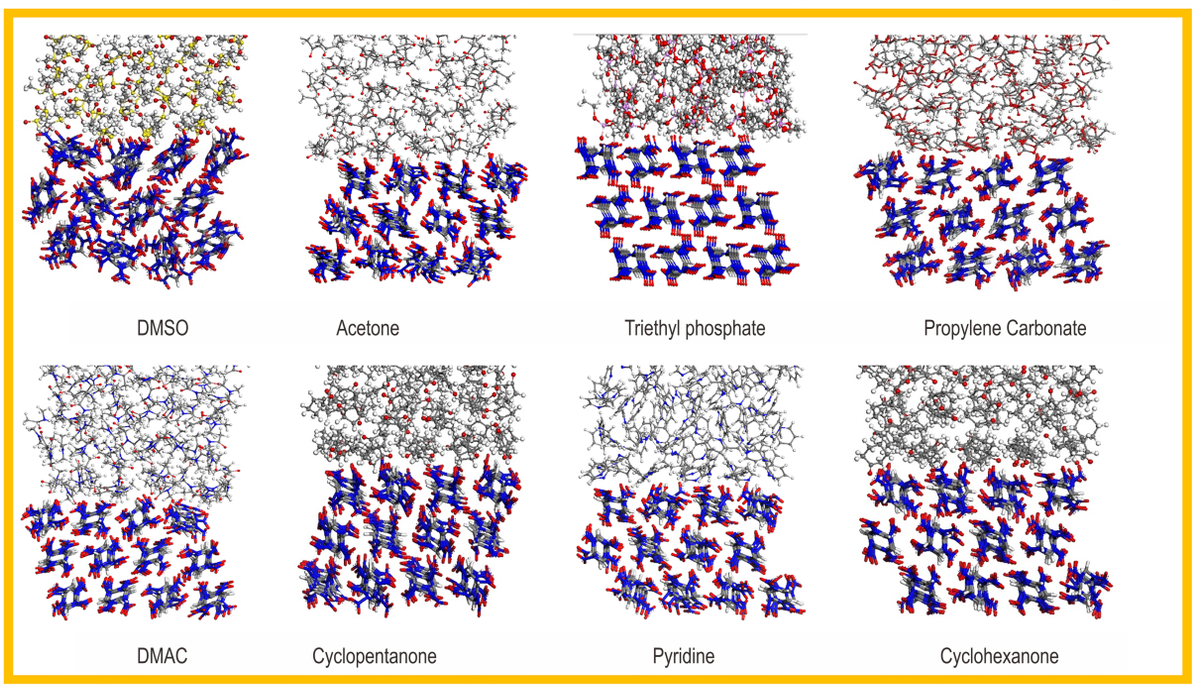

Fig.4 The equilibrium configurations of the surface-solvent molecule adsorption model structures after molecular dynamics calculations of (0 1 1) crystal face

solvent binding energy (E_s) of (1 0 0) crystal face are the largest, which is −1135.694 kJ·mol^{-1} and −180.467 kJ·mol^{-1}, respectively. This result may be due to the preferential adsorption of polar solvents on polar surfaces. The ideal morphology of HMX in vacuum showed that the (1 0 0) face is the roughest and has the strongest polarity, which results in solvent molecules are preferentially adsorbed at (1 0 0) face. A dense layer of DMSO molecules will be formed on the (1 0 0) plane, which leads to higher energy barriers for HMX molecules in solution to continue to grow on this face. Therefore, the (1 0 0) face will grow slowly and become the dominant crystal face in the final form. The (1 0 −2) is the flattest crystal surface, which is not conducive to the adsorption of DMSO molecules, so that solute molecules are easy to attach and grow on this surface. A faster growth rate may cause the surface to eventually disappear. The order of the solvent binding energy (E_s) of DMSO molecules to different crystal faces is as follows: (1 0 0)>(1 1 −1)>(1 0 −2)>(0 1 1)> (0 2 0). The (0 2 0) crystal face has the largest absolute value for the solvent-effected attachment energy (E_{att}'), which is 107.964 kJ·mol^{-1}. While the (0 1 1) and (1 1 −1) crystal faces have the smallest absolute values, which are 21.193 kJ·mol^{-1} and 21.641 kJ·mol^{-1}, respectively. The order of the absolute values for the solvent-effected attachment energy (E_a') is as follows: (0 2 0)>(1 0 −2)>(1 0 0)>(1 1 −1)≈(0 1 1). During the growth process, (0 2 0) and (1 0 −2) may be disappeared, which is consistent with the theoretical basis of the AE model, because the relative linear growth rate is proportional to its attachment energy. The relative area size of the important crystal face in the entire crystal morphology is: (0 1 1) > (1 1 −1) > (1 0 0). The expected crystal habit characteristics of the final morphology is shown in Fig. 5a. The aspect ratio of the predicted HMX crystal morphology in DMSO is 1.838. The comparison result shown in Fig.5a.

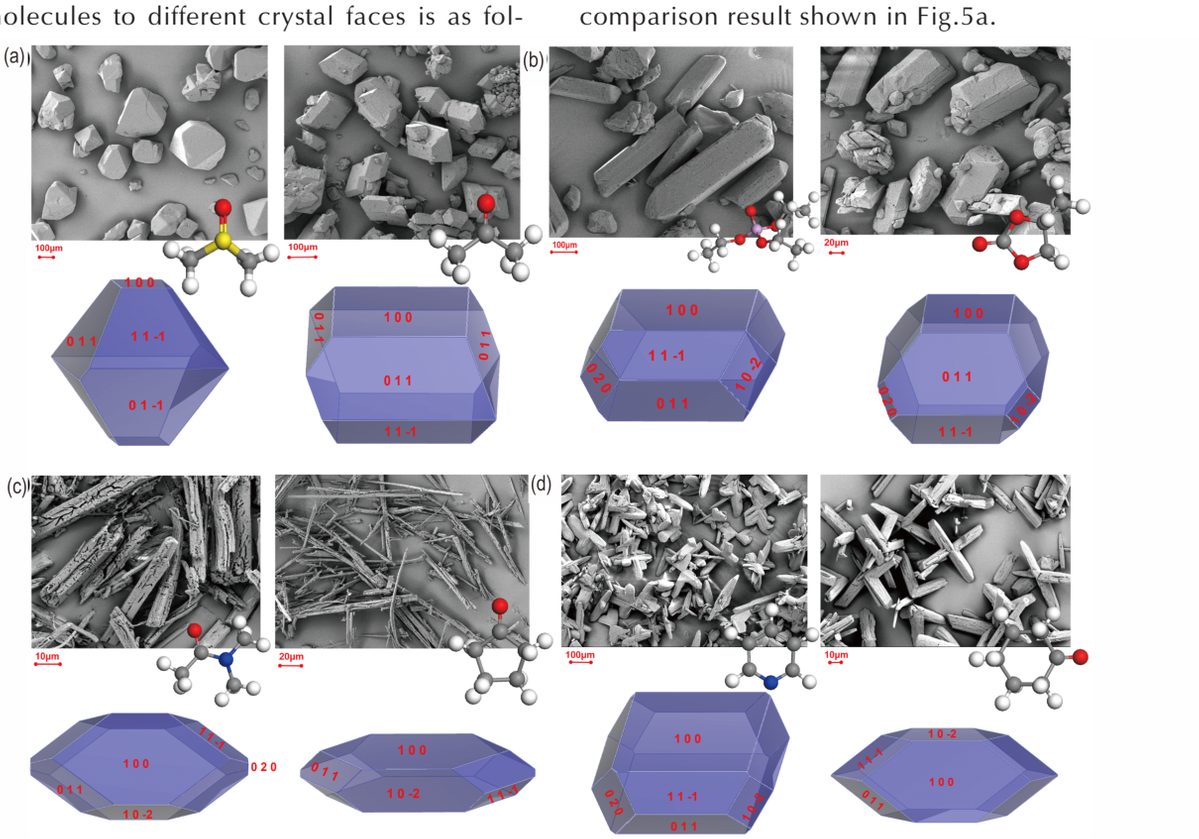

Fig.5 Simulation results by AE model and experimental crystal morphology of HMX in solvents

a—The fusiform-like crystal of HMX in DMSO and acetone, b—The rod-like crystal of HMX in Triethyl phosphate and Propylene carbonate, c—The needle-like crystal of HMX in DMAC and cyclopentanone, d—The X-like crystal of HMX in pyridine and cyclohexanone

Table 3 Calculated attachment energy for dominant crystal habit faces in different solvents

solvent	h k *l*	E_{att}	E_{int}[1]	A_{acc}	A_{box}[2]	E_s[3]	E'_{att}[4]	R[5]	total facet area/%	aspect ratio
	(0 1 1)	−110.083	−557.346	109.993	689.665	−88.889	21.193	1	50.095	
	(0 2 0)	−147.546	−598.130	62.213	940.067	−39.581	107.964	5.095	−	
DMSO	(1 1 −1)	−153.676	−788.252	126.021	752.328	−132.039	21.641	1.021	43.309	1.838
	(1 0 0)	−206.953	−1135.694	183.316	1153.620	−180.467	26.485	1.250	6.596	
	(1 0 −2)	−170.360	−919.157	132.737	1082.692	−112.687	57.673	2.722	−	
	(0 1 1)	−110.083	−13.025	109.993	689.665	−2.076	108.002	1	45.913	
	(0 2 0)	−147.546	−177.507	62.213	940.067	−11.748	135.802	1.257	−	
acetone	(1 1 −1)	−153.676	−169.355	126.021	752.328	−28.369	125.310	1.160	21.724	2.854
	(1 0 0)	−206.953	−860.206	183.316	1153.620	−136.690	70.262	0.651	32.363	
	(1 0 −2)	−170.360	−54.696	132.737	1082.692	−6.707	163.657	1.515	−	
	(0 1 1)	−110.083	−230.257	109.993	689.665	−36.722	73.356	1	29.813	
	(0 2 0)	−147.546	−603.083	62.213	940.067	−39.912	107.638	1.467	3.664	
triethyl phosphate	(1 1 −1)	−153.676	−486.401	126.021	752.328	−81.475	72.201	0.984	24.629	2.663
	(1 0 0)	−206.953	−1037.568	183.316	1153.620	−164.876	42.077	0.574	35.197	
	(1 0 −2)	−170.360	−740.184	132.737	1082.692	−90.744	79.616	1.085	6.697	
	(0 1 1)	−110.083	−190.863	109.993	689.665	−30.442	79.641	1	45.471	
	(0 2 0)	−147.546	−206.333	62.213	940.067	−13.653	133.893	1.681	1.125	
propylene Carbonate	(1 1 −1)	−153.676	−406.370	126.021	752.328	−68.068	85.607	1.075	32.915	1.849
	(1 0 0)	−206.953	−838.703	183.316	1153.620	−133.27	73.679	0.925	17.547	
	(1 0 −2)	−170.360	−572.645	132.737	1082.692	−70.204	100.156	1.258	2.943	
	(0 1 1)	−110.083	−323.656	109.993	689.665	−51.619	58.464	1	19.210	
	(0 2 0)	−147.546	−755.691	62.213	940.067	−50.011	97.539	1.668	0.701	
DMAC	(1 1 −1)	−153.676	−595.283	126.021	752.328	−99.712	53.963	0.923	20.209	3.554
	(1 0 0)	−206.953	−1128.790	183.316	1153.620	−179.370	27.582	0.472	40.273	
	(1 0 −2)	−170.360	−1043.165	132.737	1082.692	−127.889	42.470	0.726	19.607	
	(0 1 1)	−110.083	−22.018	109.993	689.665	−3.5127	106.570	1	16.803	
	(0 2 0)	−147.546	−108.651	62.213	940.067	−7.188	140.358	1.317	−	
cyclo-pentanone	(1 1 −1)	−153.676	−304.489	126.021	752.328	−51.003	102.672	0.963	12.924	4.663
	(1 0 0)	−206.953	−1038.447	183.316	1153.620	−165.014	41.939	0.394	44.185	
	(1 0 −2)	−170.360	−895.426	132.737	1082.692	−109.777	60.582	0.568	26.088	
	(0 1 1)	−110.083	−1.297	109.993	689.665	−0.205	109.874	1	25.545	
	(0 2 0)	−147.546	−27.448	62.213	940.067	−1.817	145.734	1.326	6.592	
pyridine	(1 1 −1)	−153.676	−279.590	126.021	752.328	−46.833	106.842	0.972	21.584	2.890
	(1 0 0)	−206.953	−963.671	183.316	1153.620	−153.132	53.821	0.490	41.801	
	(1 0 −2)	−170.360	−350.363	132.737	1082.692	−42.952	127.408	1.160	4.477	
	(0 1 1)	−110.083	−77.372	109.993	689.665	−12.338	97.740	1	19.552	
	(0 2 0)	−147.546	−18.769	62.213	940.067	−1.243	146.307	1.497	−	
cyclo-hexanone	(1 1 −1)	−153.676	−369.216	126.021	752.328	−61.847	91.833	0.940	18.467	3.762
	(1 0 0)	−206.953	−1002.478	183.316	1153.620	−159.299	47.654	0.488	38.389	
	(1 0 −2)	−170.360	−869.953	132.737	1082.692	−106.654	63.706	0.652	23.591	

Note: 1) The interaction energy between the solvent layer and the crystal face.2) The total crystal face area of the simulated model along the crystal face (h k *l*). 3) The binding energy of the solvent to the crystal face.4) The attachment energy of solvent influence. 5) The relative growth rates of crystal face in solvent.6) All energies are in kJ·mol^{-1}, distance in Å and area in Å^2.

4.3 Comparison of simulation and experimental results

It can be seen from Fig. 4, that the types and strengths of the bonds formed between HMX molecules and solvent molecules are different, and these differences will cause different adsorption effects of the important crystal surfaces and solvent molecules. According to the theoretical basis of the AE model (Section 2.1), the attachment energy of the crystal surface will change with the influence of solvent molecules. The crystal habit characteristics of crystal can be obtained according to the solvent-effected attachment energy. With the increase of the solvent-effected attachment energy, the growth rate of the crystal face increases. Under the continuous influence of the solvent, the crystal face with a rapid growth rate will be submerged, while the slow growing crystal face will be exposed. The final morphology of the crystal will be composed of the crystal face with small attachment energy. The interaction energy (E_{int}), solvent binding energy (E_s), solvent-effected attachment energy (E_{at}') and relative growth rate (R') of other solvent molecules and the five important crystal planes of HMX are listed in Table 3. The negative sign indicates the interaction between the solvent and the crystal surface is absorption. In the Table 3, the interaction energy (E_{int}) of the (1 0 0) face with various solvent is the highest, while the interaction energy of (1 0 −2) with various solvent molecules is relatively weak. Therefore, the dominant crystal faces of HMX are mainly (1 0 0), (0 1 1) and (1 1 −1). While (1 0 −2) is the smallest proportion area and even disappeared in various solvent. The results of the predicted HMX crystal morphologies in eight solvents are presented in Fig.5.

Recrystallization experiments of HMX were performed in the above solvents and the SEM images of the obtained recrystallized sample are shown in Fig. 6, which can be divided into four types: fusiform-like crystal (Fig.5a), rod-like crystal (Fig. 5b), needle-like crystal (Fig. 5c) and X-like crystal (Fig.5d).

Fig.6 is the power X-ray diffraction of recrystallized HMX samples. The results show that all recrystallized samples are β-HMX. The prediction results are in good agreement with the experimental samples except for pyridine and cyclohexanone. As shown in Fig. 5d, the HMX samples recrystallized from pyridine and cyclohexanone are twinnings. Twinnings are a type of surface defect, while the AE model predicts the morphology of crystal under ideal conditions. Thus the experimental samples recrystallized in pyridine and cyclohexanone are not completely consistent with the predicted results by AE model. The results of theoretical predictions indicate the trend of crystal growth of HMX in solvents and only are used as a reference, because only the effects of solvents and thermodynamics are studied, and these effects factors are very limited. In the actual recrystallization experiments, the kinetic factors and other external factors also play important roles in the morphology of HMX, such as stirring intensity, cooling rate, super-saturation and impurities.

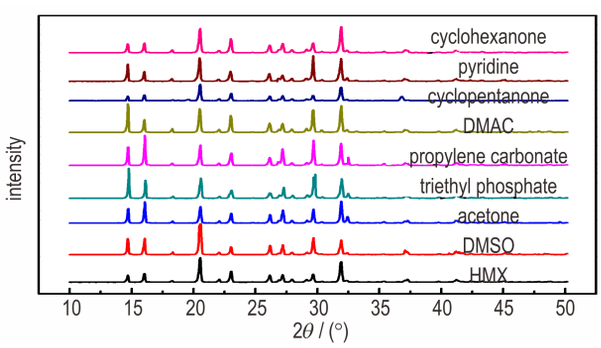

Fig.6 The power X-ray diffraction of the HMX recrystallized in eight solvents

The total facet area (%) of HMX crystal surfaces in vacuum and eight solvents are shown in Fig.7. In general, the crystal morphology of HMX is affected by solvent effects compared with that in vacuum. The area of (0 1 1) face decreased while the area of (1 0 0) face increased in all solvents. The (0 2 0) face area decreases in all solvents and even disappears in DMSO, acetone, cyclohexanone and cyclopentanone. The area of (1 0 −2) face increases except for DMSO and acetone. (0 1 1) faces occupy a relatively large area. It can be seen that the crystal morphology of HMX in vacuum and in triethyl phos-

phate, propylene carbonate, DMAC and pyridine dominated by five faces, while there are only four faces in cyclopentanone and cyclohexanone, and three faces in DMSO and acetone. For particle morphology, the aspect ratio can be used to determine whether the shape is close to spherical. The aspect ratio is defined as the ratio between the longest and shortest diameters of habit. The aspect ratio value is close to 1, indicating that the morphology of HMX tends to be more spherical. The aspect ratio is the result of the interaction of various solvent molecules with all important crystal faces. The aspect ratio values of the predicted HMX crystal morphology in different solvents are listed in Table 3, and the order of the aspect ratio is: cyclopentanone > cyclohexanone > DMAC > pyridine > acetone > triethyl phosphate > propylene carbonate > DMSO. The smaller the aspect ratio of the crystal morphology, the closer the crystal morphology to the cube, recrystallization of HMX in this solvent is more conducive to the spheroidization.

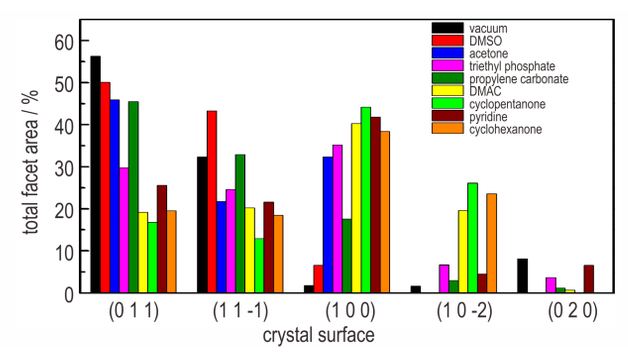

Fig.7 The total facet area of HMX crystal surfaces in vacuum and eight solvents

5 Conclusion

In this work, the MD simulations of HMX in eight solvents including dimethyl sulfoxide (DMSO), acetone, triethyl phosphate, propylene carbonate, *N*, *N*-dimethylacetamide (DMAC), cyclopentanone, cyclohexanone and pyridine systems were performed to obtain the attached energy between the solvent molecules and the dominant crystal face. Different morphologies of HMX crystal were obtained by using the attached energy (AE) model.

(1) The dominant crystal faces of HMX in vacuum are (0 1 1), (1 1 −1), (0 2 0), (1 0 0) and (1 0 −2). The (1 0 0) face is the most polar crystal face and has the largest interaction energy with the solvent molecules. Hence, it has a slower growth rate and appears as dominant surfaces in the final crystal morphology. And (1 0 −2) and (0 2 0) are crystal faces with large attached energy, which appear as the smallest area or even disappears in the final crystal morphology.

(2) The crystal morphology of HMX is affected by solvent effects. The area of different crystal faces is changed with the variation of the solvent. The order of the aspect ratio of the crystal morphology in eight solvents is: cyclopentanone>cyclohexanone > DMAC > pyridine > acetone > triethyl phosphate > propylene carbonate > DMSO. The smaller the aspect ratio of the crystal morphology is in DMSO and propylene carbonate, the closer the crystal morphology is to the cube or spherical and the higher packing density. Recrystallization of HMX in DMSO is more conducive to spheroidization, which will be more beneficial to the subsequent use of HMX.

(3) The recrystallization experiments results show that all of the recrystallized samples are β-HMX. The prediction results are in good agreement with the experimental results. The attached energy (AE) model is suitable for predicting the crystal habit of HMX, which can guide the HMX crystal morphology control by recrystallization experiments.

References:

[1] Zhang Chaoyang, Ji Chunliang, Li Hongzhen, et al. Occupancy model for predicting the crystal morphologies influenced by solvents and temperature, and its application to nitroamine explosives[J]. *Crystal Growth & Design*, 2013,13(1): 282−290.

[2] Song Xiao-lan, Guo Xiao-de, Zhang Jing-lin, et al. Dependence of size and size distribution on safety performance of nitroamine explosives and the multi-component explosives[J]. *Initiators and Pyrotechnics*, 2007,4 (116): 17.

[3] Kröber Hartmut, Teipel Ulrich. Crystallization of insensitive HMX[J]. *Propellants, Explosives, Pyrotechnics: An International Journal Dealing with Scientific and Technological Aspects of Energetic Materials*, 2008,33 (1): 33−36.

[4] Vaullerin Maryse, Espagnacq André , Morin-Allory Luc. Prediction of explosives impact sensitivity[J]. *Propellants, Explo-*

sives, *Pyrotechnics*, 1998,23(5): 237-239.
[5] Oxley Jimmie, Smith James, Buco Robert, et al. A study of reduced-sensitivity RDX [J]. *Journal of Energetic Materials*, 2007,25(3): 141-160.
[6] Sivabalan R, Gore G M, Nair U R, et al. Study on ultrasound assisted precipitation of CL-20 and its effect on morphology and sensitivity[J]. *Journal of Hazardous Materials*, 2007, 139 (2): 199-203.
[7] Song Xiaolan, Wang Yi, An Chongwei, et al. Dependence of particle morphology and size on the mechanical sensitivity and thermal stability of octahydro-1, 3, 5, 7-tetranitro-1, 3, 5, 7-tetrazocine[J]. *Journal of Hazardous Materials*, 2008, 159 (2-3): 222-229.
[8] Zhang Chaoyang, Peng Qiang, Wang Liyan, et al. Thermal sensitivity of HMX crystals and HMX-Based explosives treated under various conditions[J]. *Propellants, Explosives, Pyrotechnics*, 2010,35(6): 561-566.
[9] Ter Horst J H, Geertman R M, Van der Heijden A E, et al. The influence of a solvent on the crystal morphology of RDX[J]. *Journal of Crystal Growth*, 1999,198(1): 773-779.
[10] Cockrem M C M. Crystallization technology handbook[M]. New York: 1996.
[11] Bravais A. Etudes Crystallographiques[M]. Paris: Gauthier-Villars, 1866.
[12] Friedel Georges. Etudes sur la loi de Bravais[J]. *Bulletin de Minéralogie*, 1907,30 (9): 326-455.
[13] Donnay J_D H, Harker David. A new law of crystal morphology extending the law of Bravais[J]. *American Mineralogist: Journal of Earth and Planetary Materials*, 1937, 22 (5): 446-467.
[14] Hartman Piet, Perdok W G. On the relations between structure and morphology of crystals. I[J]. *Acta Crystallographica*, 1955,8(1): 49-52.
[15] Hartman P, Bennema P. The attachment energy as a habit controlling factor: I. Theoretical considerations[J]. *Journal of Crystal Growth*, 1980,49(1): 145-156.
[16] Hartman P. The attachment energy as a habit controlling factor II. Application to anthracene, tin tetraiodide and orthorhombic sulphur[J]. *Journal of Crystal Growth*, 1980,49(1): 157-165.
[17] Winn Daniel, Doherty Michael F. Predicting the shape of organic crystals grown from polar solvents[J]. *Chemical Engineering Science*, 2002,57(10): 1805-1813.
[18] Lu J J, Ulrich J. An improved prediction model of morphological modifications of organic crystals induced by additives[J]. *Crystal Research and Technology: Journal of Experimental and Industrial Crystallography*, 2003,38(1): 63-73.
[19] Berkovitch-Yellin Ziva. Toward an ab initio derivation of crystal morphology[J]. *Journal of the American Chemical Society*, 1985,107(26): 8239-8253.
[20] Deij M A, Meekes H, Vlieg E. The step energy as a habit controlling factor: application to the morphology prediction of aspartame, venlafaxine, and a yellow isoxazolone dye[J]. *Crystal Growth & Design*, 2007,7(10): 1949-1957.
[21] Han Gang, Zhang Shu-hai, Gou Rui-jun, et al. Comparative study of solvent-CL-20 interactions at different roughness crystal surfaces: Molecular dynamics simulation[J]. *Computational and Theoretical Chemistry*, 2018,1136:49-55.
[22] Song Liang, Chen Lizhen, Wang Jianlong, et al. Prediction of crystal morphology of 3, 4-dinitro-1H-pyrazole (DNP) in different solvents[J]. *Journal of Molecular Graphics and Modelling*, 2017,75:62-70.
[23] Liu Yingzhe, Lai Weipeng, Yu Tao, et al. Understanding the growth morphology of explosive crystals in solution: insights from solvent behavior at the crystal surface[J]. *RSC Advances*, 2017,7(3): 1305-1312.
[24] Chen Fang, Zhou Tao, Li Jun, et al. Crystal morphology of dihydroxylammonium 5, 5′-bistetrazole-1, 1′-diolate (TKX-50) under solvents system with different polarity using molecular dynamics[J]. *Computational Materials Science*, 2019, 168: 48-57.
[25] Czerski H, Greenaway MW, Proud W G, et al. β-δ phase transition during dropweight impact on cyclotetramethylene-tetranitroamine[J]. *Journal of Applied Physics*, 2004, 96 (8): 4131-4134.
[26] Cady Howard H. Studies on the Polymorphs of HMX[R], LAMS-2652: 1962.
[27] Goldberg Ilana G. Directed crystal growth and solid-state analysis of the secondary explosives RDX and HMX[D], Washington D.C.: Georgetown University, 2011.
[28] Svensson Leif, Nyqvist Jan-Olof ,Westling Lars. Crystallization of HMX from γ-butyrolactone[J]. *Journal of Hazardous Materials*, 1986,13(1): 103-108.
[29] van der Heijden Antoine E D M , Bouma Richard H B. Crystallization and characterization of RDX, HMX, and CL-20[J]. *Crystal Growth & Design*, 2004,4(5): 999-1007.
[30] Duan Xiaohui, Wei Chunxue, Liu Yonggang, et al. A molecular dynamics simulation of solvent effects on the crystal morphology of HMX[J]. *Journal of Hazardous Materials*, 2010, 174(1-3): 175-180.
[31] Tao Jun , Wang Xiaofeng. Crystal structure and morphology of β-HMX in acetone: A molecular dynamics simulation and experimental study[J]. *Journal of Chemical Sciences*, 2017,129 (4): 495-503.
[32] Yan Tao, Wang Jian-Hua, Liu Yu-Cun, et al. Growth and morphology of 1, 3, 5, 7-tetranitro-1, 3, 5 7-tetraazacy-clooct ane (HMX) crystal[J]. *Journal of Crystal Growth*,2015,430: 7-13.
[33] Chen Fang, Liu Yuan-Yuan, Wang Jian-Long, et al. Nvestigation of the co-solvent effect on the crystal morphology of β-HMX using molecular dynamics simulations[J]. *Acta Physico-Chimica Sinica*, 2017,33(6): 1140-1148.
[34] Liu Ning, Li Ya-nan, Zeman Svatopluk, et al. Crystal morphology of 3, 4-bis (3-nitrofurazan-4-yl) furoxan (DNTF) in a solvent system: molecular dynamics simulation and sensitivity study[J]. *CrystEngComm*, 2016,18(16): 2843-2851.
[35] Chen Jie ,Trout Bernhardt L. Computer-aided solvent selection for improving the morphology of needle-like crystals: A case study of 2, 6-dihydroxybenzoic acid[J]. *Crystal Growth & Design*, 2010,10(10): 4379-4388.
[36] Sun Huai. COMPASS: an ab initio force-field optimized for condensed-phase applications overview with details on alkane and benzene compounds[J]. *The Journal of Physical Chemistry B*, 1998,102(38): 7338-7364.
[37] Cady Howard H, Larson Allen C ,Cromer Don T. The crystal structure of α-HMX and a refinement of the structure of β-HMX [J]. *Acta Crystallographica*, 1963,16(7): 617-623.

八种溶剂体系中HMX晶体形貌的分子动力学模拟和实验研究

王 蕾[1,2],陈 东[2],李洪珍[2],段晓惠[3],于雁武[1]

(1. 中北大学环境与安全工程学院, 山西 太原 030051; 2. 中国工程物理研究院化工材料研究所, 四川 绵阳 621999; 3. 西南科技大学化工学院, 四川 绵阳 621999)

摘 要: 采用附着能模型(AE模型)和分子动力学方法(MD方法)预测了奥克托今(HMX)在八种常用有机溶剂中的重结晶形态。结果表明,在真空中预测得到HMX晶体形态的优势晶面分别为:(0 1 1),(1 1 -1),(0 2 0),(1 0 0)和(1 0 -2)。其中(1 0 0)面是极性最大的晶面,并且与溶剂分子的相互作用能最大,因而导致该面的生长速度变慢,并在最终的晶体形态中成为面积较大的优势面。(1 0 -2)和(0 2 0)是与溶剂分子具有较小相互作用能的晶体面,在最终的晶体形态中这两个面表现为面积最小的晶面甚至是消失。计算了晶体形态的长径比,其顺序为:环戊酮>环己酮>*N*,*N*-二甲基乙酰胺(DMAC)>吡啶>丙酮>磷酸三乙酯>碳酸丙烯酯>二甲基亚砜(DMSO),这表明在二甲基亚砜和碳酸丙烯酯中进行重结晶实验更有利于HMX的球化。采用自然冷却方法在八种纯有机溶剂中对HMX进行了重结晶实验,重结晶实验结果与AE模型的模拟结果吻合良好,这表明AE模型适用于预测HMX的晶体形态,对HMX重结晶实验具有指导作用。

关键词: 附着能(AE)模型;β-HMX;晶体形态;分子动力学;模拟

中图分类号: TJ55; O64 **文献标志码:** A **DOI:** 10.11943/CJEM2020019

(责编:王艳秀)